Proceedings of
11th European Conference on Turbomachinery Fluid dynamics & Thermodynamics
ETC11, March 23-27, 2015, Madrid, Spain

DESIGN OF NEXT GENERATION SNOW GUN FANS

A. Corsini[1] – G. Delibra[1] – F. Sciulli[2]
[1]Dipartimento di Ingegneria Meccanica e Aerospaziale, Sapienza Università di Roma, Italy
alessandro.corsini@uniroma1.it - giovanni.delibra@uniroma1.it
[2]SED Soluzioni per l'Energia e la Diagnostica Srl, Ferentino (FR), Italy
fabrizio.sciulli@sedsoluzioni.com

ABSTRACT

Most of the skiing resorts normally use snow guns to ensure a suitable amount of artificial snow on ski tracks. The main component of a snow gun are a fan used to move the air and an atomizer to inject droplets of water in the main flow. Issues with these devices are (i) power requirements, between 10 and 30 kW for a single device (a complete track needing up to 100 snow guns) and (ii) acoustic emissions, typically above 80 dB due to the rotational speed comprised between 1500 and 3600 rpm. The paper describes the development of a family of next-generation snow gun to cover a wide range of applications. The design process is based on a methodology that combines Eulerian analysis, RANS computations and experiments.

NOMENCLATURE

latin

C	chord [m]
D	diameter [m]
DF	diffusion factor [-]
P	power [W]
Q	volume flow rate [m^3/s]
R	radius [m]
U	tangential velocity [m/s]
V	absolute velocity [m/s]
W	relative velocity [m/s]
Z	number of blades [-]

greek

ρ	density [kg/m^3]
σ	solidity [-]
ω	rotational velocity [rpm]
ζ	losses [-] $\zeta=[p_{tot}^{(in)} - p_{tot}]/ [0.5\rho (W^{in})^2]$

superscript / subscripts

in	average value of a quantity at the inflow
rot	quantity refers to rotor of the fan
stat	quantity refers to stator of the fan

INTRODUCTION

Snow guns were developed and used over the last fifty years on ski resort to produce artificial snow. The use of snow guns allowed to extend the skiing season and to regulate the quality of snow on ski tracks. Main components of snow guns are i) a jet fan fitted to a convergent casing that provides air, and ii) an atomizer that sprays water droplets in the main jet at the exit of the snow gun.

A key aspect in snow gun devices is the coupling of the fan and the atomizer; in fact liquid water injected into the main flow core of the snow gun need to be turned into snow in the small amount of time that passes from the injection to landing onto the ski track. In snow gun operations it is essential to guarantee that all the water injected is turned into snow (to avoid feeding tracks with wet snow not suitable for skiing) and to maximize the quantity of water injected to increase the efficiency of the process. Chen and Kevorkian (1971) investigated the mixing of water and compressed air in a snow nozzle, focusing on the pressure of injection of air and water and the ratio between water and air mass flows. Strub et al. (2003) scrutinized the modelling of crystallization of water droplets basing their models on an available experimental database that accounted for a three-stage transformation from super-cooled liquid phase to liquid-solid phase to solid phase. Hanzer et al. (2014) implemented and

validated a module for the simulation of artificial snow production on a ski area of known characteristics considering individual snow guns, real-geometry mountain slopes and realistic thermodynamics conditions. As the growth of snowflakes needs to be very fast to avoid wet snow on tracks, it is common practice to seed water with ice nucleators. Liao and Ng (1990) studied the effect of ice nucleators derived from bacteria on the efficiency of snow making, extending the theory of nucleation spectrum to account for variation of nucleation temperature of water droplets and applying such approach to snow guns. Lagriffoul et al. (2010) assessed the health and environmental risks related to the use of bacteria as ice nucleators for artificial snow production.

In this paper we focus on the design of a new fan to replace the one inside a state-of-the-art snow gun (labelled as *D800*). For industrial purposes it was assumed that no changes were possible with respect to the atomizer.

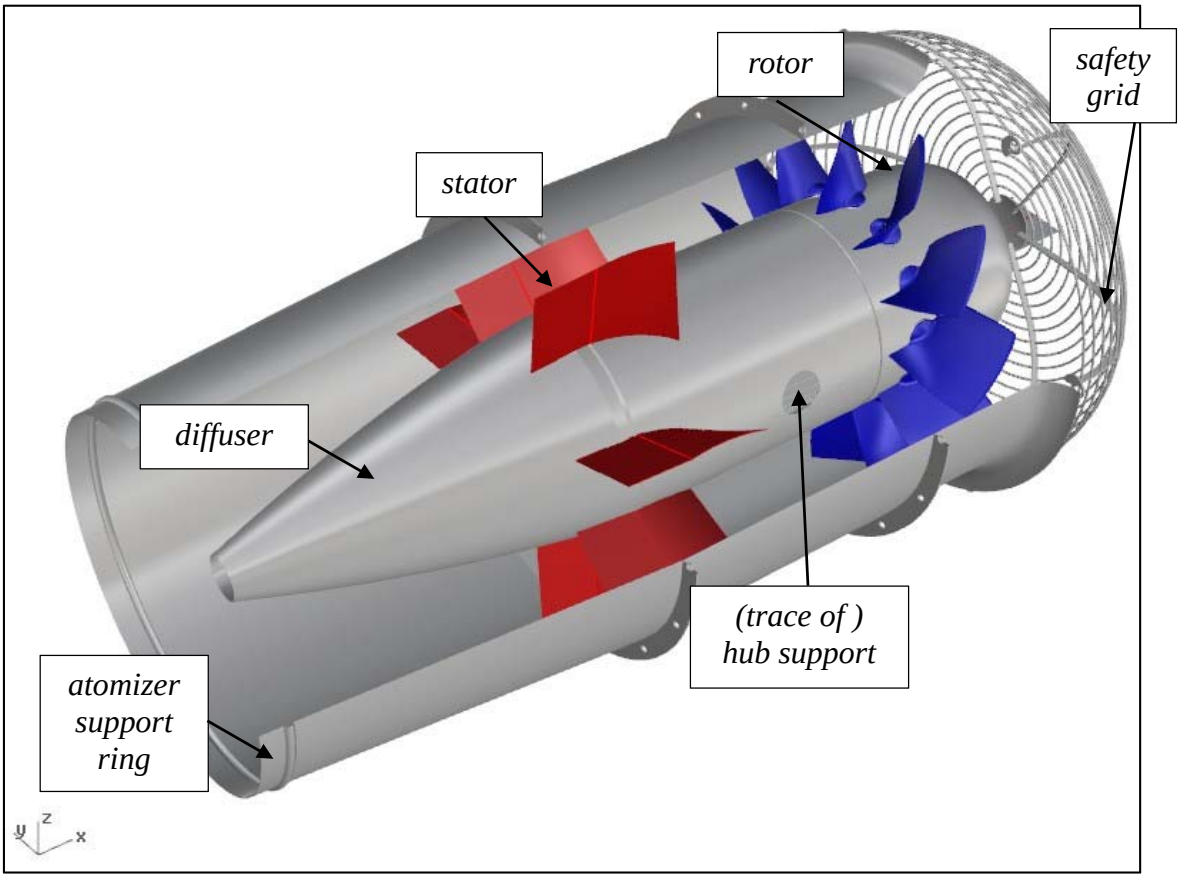

Figure 1 - An overview of the D800 snow gun. Blue: rotor, red: stator – courtesy of Fieni s.r.l.

DATUM GEOMETRY AND DESIGN SPECIFICATIONS

DATUM CONFIGURATION – *D800*

The datum geometry for the fan is shown in Figure 1. The *D800* unit is composed of a safety grid that prevent direct access to a 12 blades rotor and a 7 blades stator. Here the stage has a peculiar arrangement so that the stator is placed 410 mm downstream of the rotor (as a reference the midspan chord of the rotor is C_{ROTmid} = 0.19 m).

The casing of the fan has a bended profile at the inlet to facilitate the inflow of air, followed by a constant section with a 800 mm diameter and a slightly convergent cross-section at the exit where an atomizer (not shown in figure) is fitted. The hub of the fan has a spinner cone at the inflow and a 400mm diameter and a convergent diffuser-like shape at the outflow. The motor of the fan is fitted

inside the hub. The hub is fixed to the casing with a support that includes also the electric cables for power and management of the unit. Rotational speed of the fan is set to 1450 rpm.

The specifications of the fan are summarized in Table 1.

Table 1 – D800 fan blade data and corresponding D800⁺ design specs

	D800		**D800+ design specs**
D_{casing}	800 mm		800 mm
D_{hub}	400 mm		800 mm
Tip clearance	5 mm		5 mm
Z_{rot}	12		≤12
Z_{stat}	7		*not specified*
ω	1450 rpm		1450 rpm
Q	11.55 m^3/s		11.55 m^3/s
	hub	*tip*	
C	165 mm	172 mm	*not specified*
σ	1.48	0.84	*not specified*

Design specifications for *D800⁺*

The present work was carried out aiming at an increase of aerodynamic efficiency of the fan, a reduction of D800 capital and operational costs. This was achieved designing a new rotor blade and reducing the number of blades. By-product objective was the reduction of acoustic emissions valued by the manufacturer. Design constraints of the optimized *D800⁺* fan were the necessity to fit the fan to the same frame of *D800*, so that the hub and tip diameter were to stay constant and to use the same motor, so to keep constant angular velocity of the fan. Finally, in order to ensure proper coupling with the atomizer, the volume flow rate and velocity profile at the exit of the snow gun needed to remain constant.

METHODOLOGY

Eulerian analysis

Eulerian analysis was carried out with the in-house TLab solver. The rotor blade was discretized with 11 2D profiles taken along the span at constant spacing. The solver was able to derive the geometrical quantities for Eulerian analysis of the *D800* datum configuration.

CFD analysis

To validate the performance of the geometry generated by TLab a CFD analysis was carried out with OpenFOAM 2.3.x, a finite volume open-source C++ library for computations of turbulent flows.

Given the peculiar rotor-stator arrangement, with the stator more than 2 rotor chords downstream of the rotor, the simulation was handled neglecting a full coupling of rotor and stator.

The flow field in the rotor of the domain, Figure 2, was simulated in steady-state mode, entailing only one blade passage and using periodicity at mid-pitch. Computations were carried out in the rotating frame of reference, accounting for the effects of centrifugal and Coriolis forces into momentum equations. The set of boundary conditions for the simulation is summarized in Table 2.

The simulation of the stator, Figure 3, was carried out in unsteady mode, taking the absolute velocity, k and ε fields from the simulation of the rotor and rotating it at each timestep, Table 3.

Results for the stator computations were averaged over 1.2 revolution of the rotor. Details on the fully hexahedral grid of the rotor and the fully tetrahedral grid of the stator are given in Table 4.

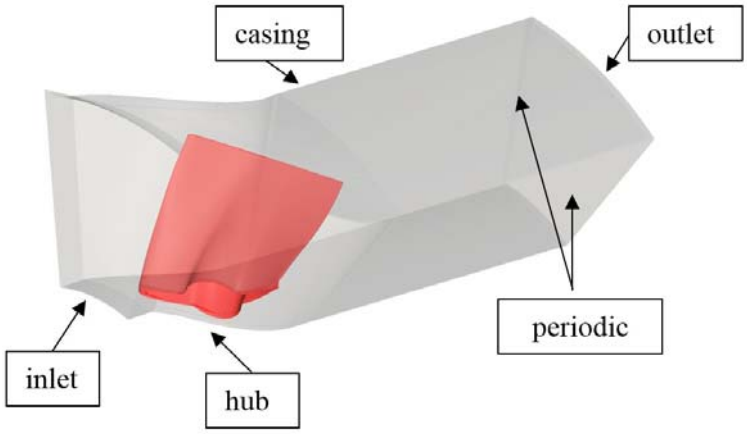

Figure 2 – Rotor, computational domain

Time integration was based on 2nd order Crank Nicholson scheme for the stator computations, while the rotor's were carried out in steady state mode. In both computations, the convection terms were discretized using TVD scheme. Turbulence closure was based on the low-Reynolds non linear formulation of the k-ε model of Lien and Leschziner (1994). Convergence threshold of the solver for all quantities was set to 10^{-8}.

Table 2 - Boundary conditions for rotor computation

Inflow	Velocity profile (Sheard et al., 2009), TI = 5%
Outflow	zeroGradient
Rotor	No-slip
Stator	V=ωR
Periodic boundaries at mid-pitch	

Table 3 - Boundary conditions for stator computations

Inflow	Velocity, k, e profiles from rotor simulation
Outflow	zeroGradient on all quantities
Solid walls	No-slip

Table 4 - Fan mesh data

	rotor	*stator*
Number of cells	$3x10^6$	$3x10^7$
Average y^+	1.2	1.9
Average cell aspect ratio	1.3	1.2

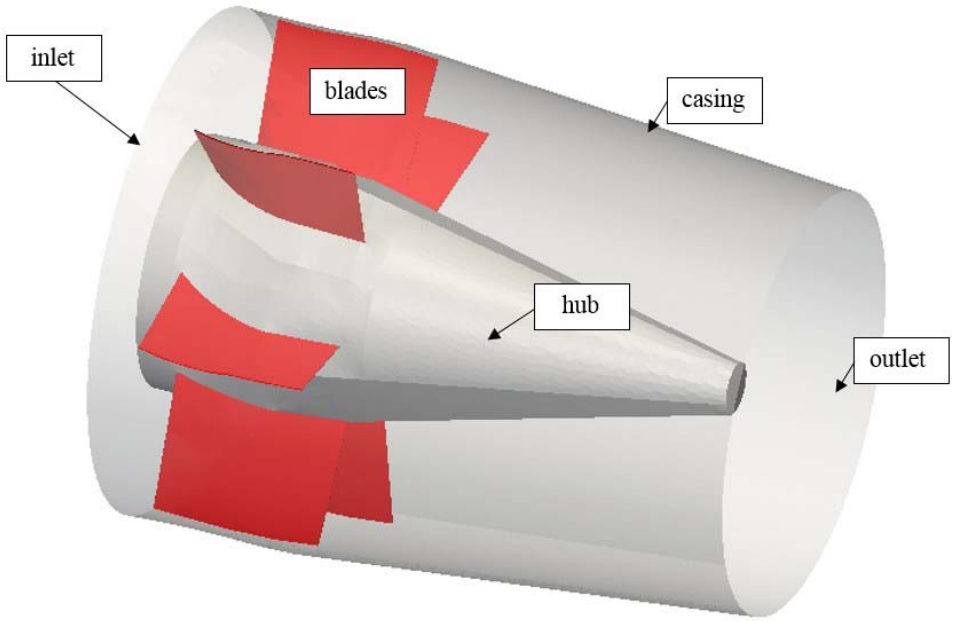

Figure 3 – Stator, computational domain

DEVELOPMENT OF NEW GEOMETRY

D800 flow survey

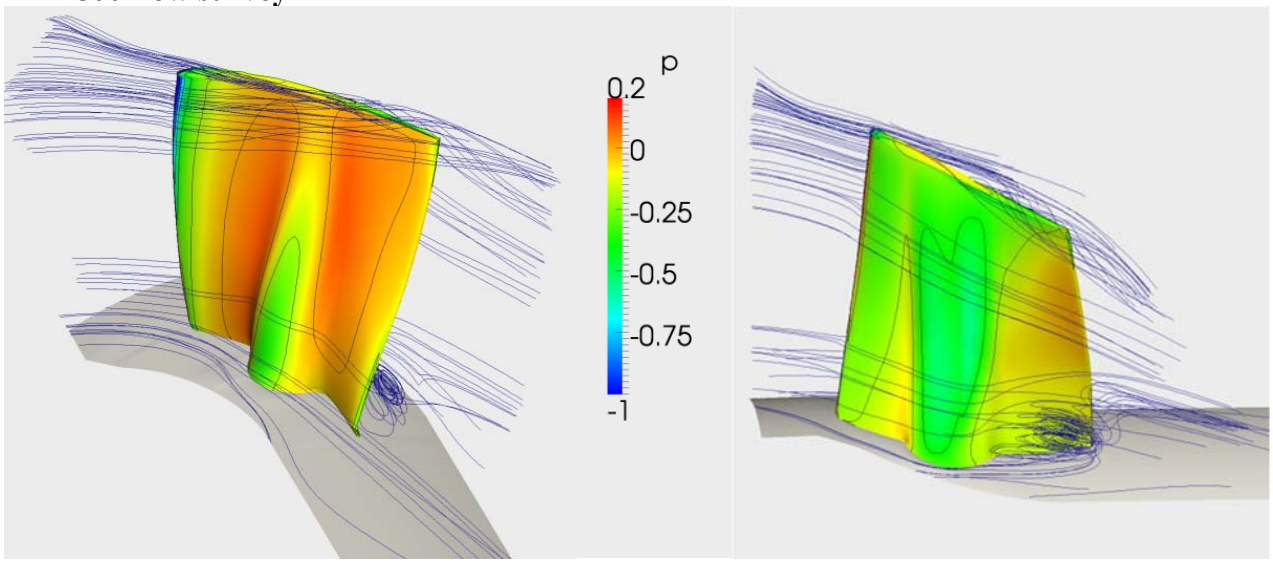

Figure 4 – D800 rotor, three-dimensional streamlines and normalized pressure contour over the blade surface. Left: pressure side, right: suction side. In both figures the flow is moving from left to right

Part of the challenge of the present project was to deal with a blind test case. In fact it was known that the D800 configuration was able to correctly produce high quality snow, but no information was available with respect to the distribution of velocity and turbulence intensity at the exit of the snow gun. These data were essential in order to correctly couple the flow with the atomizer. It was therefore necessary to reconstruct this piece of information with numerical computations.

The same numerical investigation was exploited to investigate possible ways to increase the efficiency of the fan and reduce the cost of the single fan unit. Numerical results were compared

against available measurements, and were able to predict the total pressure rise of the fan with a 2% accuracy. Aerodynamic power overestimated the electric power by 7.5%. Considering a further loss of efficiency due to mechanical and electrical efficiencies it was possible to assess that the prediction was sufficiently accurate.

In

Figure 4 an overview of the rotor flow field is given. The typical leakage vortex is recognizable at the tip of the fan. The other main recognizable structure is a separation zone at the hub of the fan that is released on the suction side due to the peculiar blunt shape of the stud of the rotor. In Figure 5 velocity and losses contours in a cross-section 0.2 chords downstream of the rotor are shown, highlighting the correlation between the hub separation and losses.

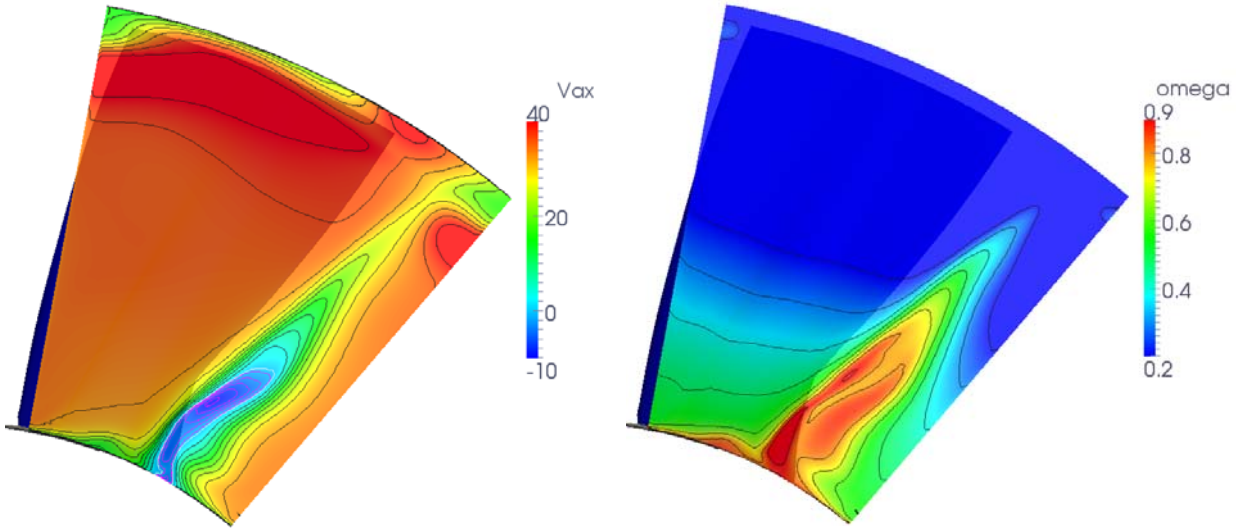

Figure 5 – Axial velocity in [m/s] (left) and losses (right) contours onto an axial cross-section taken 0.2 chords downstream of the rotor. On the left the purple contour encloses the recirculation zone.

The main outcome of the stator simulation was the presence of a large separation zone in the lower half of the blade span, Figure 6. This separation was generated by the not correct alignment of the stator leading edge with the incoming flow field released by the rotor. Finally the computation provided the piece of information necessary to understand what kind of velocity profile at the exit of the snow gun was able to provide the correct matching with the atomiser (discussed below).

Eulerian analysis of D800 and reverse engineering of D800$^+$ geometry

The analysis of the datum D800 geometry allowed to derive the geometrical quantities for Eulerian analysis and the distribution of Euler's work along the span of the blade. To this aim the blade was divided into 10 control profiles equally spaced along the radius that in the following are labelled as radial positions 1 to 10 (1 being at the hub, 10 at the tip of the blade). In Figure 7 is shown the radial distribution of Euler work along the blade of D800 configuration. Following the consideration of flow field analysis and in particular the low level of losses and the radial distribution of DF shown in the same figure, we concluded that it was possible to increase the work at the tip of the blade, and imposed a new distribution to derive a D800$^+$ geometry (shown in red in the same figures). The solver generated a geometry with this distribution of work increasing the chord at the tip of the blade and changing the camber of the profiles. As one of the aims of the process was to decrease the costs of the fan, the solver generated a geometry accounting for a blade reduction from

12 to 6 accounting for a re-staggering of the rotor blade. The new distribution of chord and solidity are shown in Figure 8, and compared with those of D800 rotor geometry.

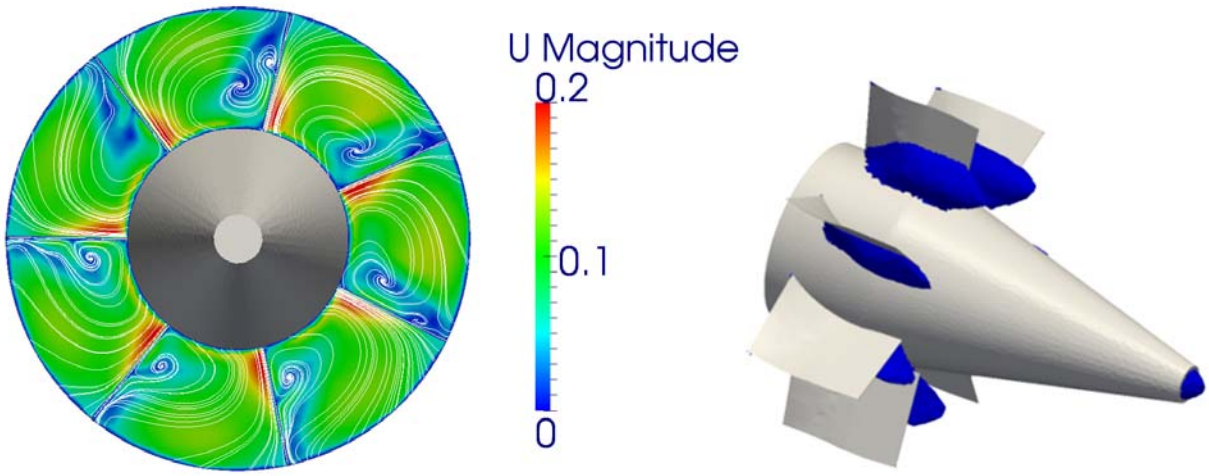

Figure 6 – Stator, normalized velocity magnitude contours onto an axial cross-section at 50% of the stator blade with 2D streamlines (left) and 3D separations highlighted in blue (right)

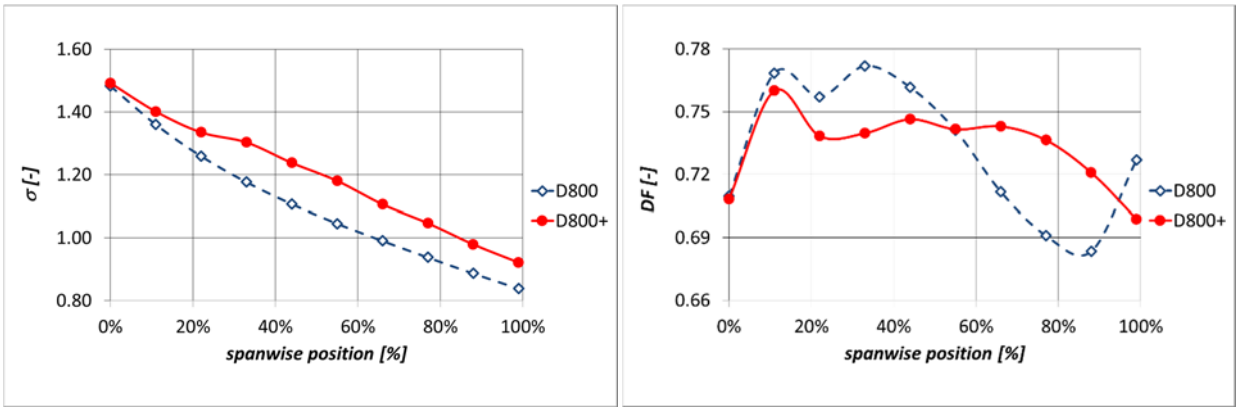

Figure 7 – Radial distributions of Euler work (left) and DF (right) for D800 (blue) and D800⁺ (red) rotor blades

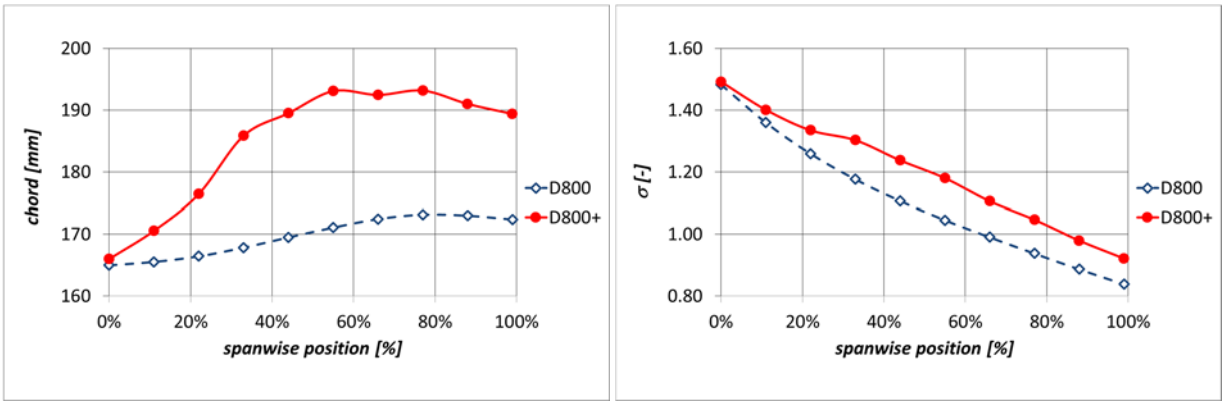

Figure 8 – Radial distributions of chord (left) and solidity (right) for D800 (blue) and D800⁺ (red) rotor blades

D800⁺ flow survey

The new D800⁺ geometry derived through inverse design was numerically tested with the same methodology applied for the D800. The numerical analysis lead to a reduction of the power of 1.2kW with respect to the D800 numerical power. Moreover it was possible to derive a velocity profile at the

exit of the rotor and to re-design the leading edge of the stator in order to avoid separation of the flow as for D800 geometry. In Figure 9 a survey of the flow in the rotor is given. The main difference with the datum configuration is in the lack of hub separation due to the smoother profile without the stud.

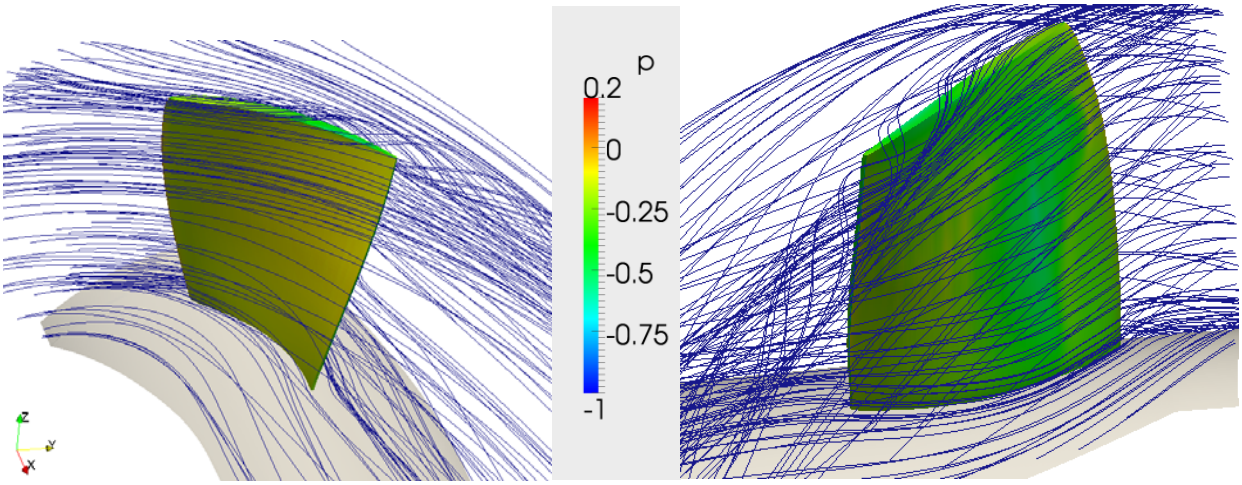

Figure 9 – D800+ rotor, three-dimensional streamlines and normalized pressure contour over the blade surface. Left: pressure side, right: suction side. In both figures the flow is moving from left to right

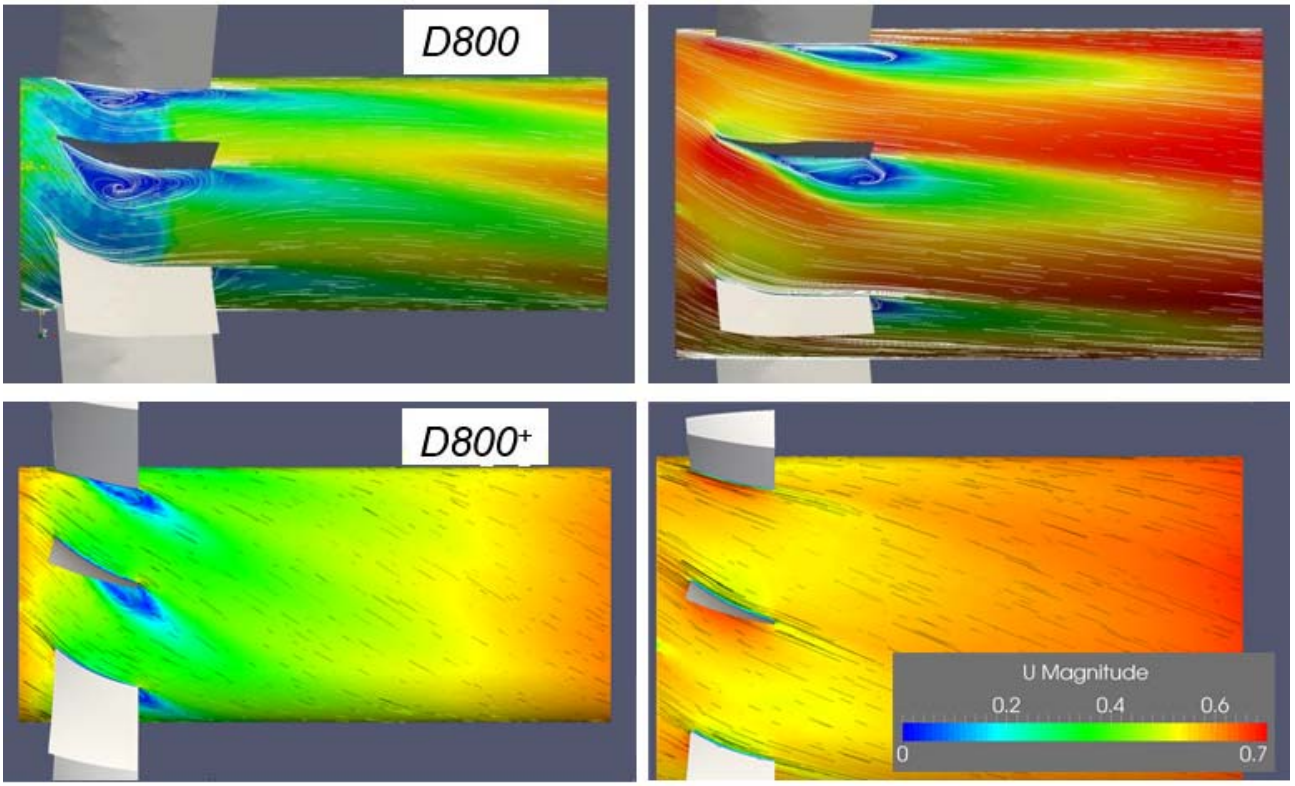

Figure 10 – Normalised velocity contours with streamlines at 5% (left) and 50% of the blade span for D800 (top) and D800+ (bottom)

In Figure 10 velocity contours and streamlines in the stator are shown at 5% and 50% of the radial span for D800 and D800$^+$ geometries. In both cases separation occurs near the hub of the fan, but in the D800 geometry it is limited to that portion of the blade span, as at midspan the flow is completely attached. Design of the stator was carried out using the angle-of-attack computed by CFD assuming

to have a completely axial direction of the flow at the trailing edge. Increase of the number of blades from 7 to 14 was not accepted by the manufacturer due to increase of costs.

Prototype test

The D800^{+} geometry was finally assembled and tested on the field, confirming that the snow gun was able to correctly producing the same amount of snow with the same quality. The new geometry lead to a 1.1 kW reduction of the electrical power absorbed from the motor and a reduction of the number of blades of the rotor from 12 to 6 (the quantity of metal necessary to produce the blades decreased of about 40%). In Figure 11 the measured axial velocity profile at the exit of D800 (averaged over 360 deg) is compared with the same of D800^{+} showing that there are only minor changes and proving the correct coupling with the snow atomizer.

Table 5 – Experimental power consumption of D800 and D800^{+}

	P	**Z_{rot}**	**dBA**	**normalised weight of rotor blade**
D800	18.5 kW	12	84.8	1
D800^{+}	17.4 kW	6	83.2	0.6
Δ	-1.1 kW	-50%	-1.6 dBA	-40%

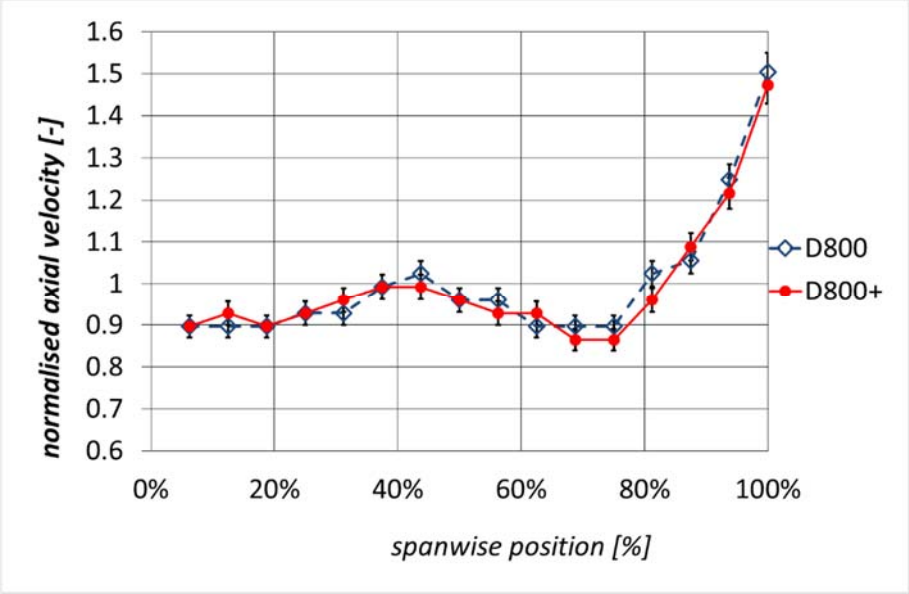

Figure 11 – Radial distribution of axial velocity at the exit of the D800 (blue) and D800^{+} (red) measured experimentally

Finally in Table 5 are summarized the differences in performance of D800 and D800+ measured in terms of power, number of blades and noise measured 1m downstream of the outlet of the nozzle.

CONCLUSIONS

In this paper we presented the reverse engineering and optimisation of the fan of a snow gun. The process was limited to the necessity to fit the fan in the same frame of the datum geometry and to the necessity to correctly coupling the jet of air at the discharge with the existing atomizer.

As the only available data were the geometry of the rotor and stator blades and the data measured by the motor (power and rotational speed) CFD and Eulerian analysis were used to study the operation of the snow gun from an aerodynamical point of view and derive possible solution to increase the

efficiency and reduce the costs of the fan. This analysis lead to the conclusion that it was possible to increase the load on the blade and that it was necessary to re-align the stator blades to match the velocity profile released by the rotor. A reduction of blade number was achieved re-staggering the new blade of by 3deg.

A new $D800^{+}$ geometry was derived and numerical investigation concluded that it lead to an increase of efficiency without altering the velocity profile at the exit of the snow gun.

Axial velocity was measured at the exit for both D800 and $D800^{+}$ confirming that the new geometry did not mess with the aerodynamic performance of the snow gun. Electric power of the $D800^{+}$ showed a 1.1kW reduction of power. Field measurements confirmed the good quality of the snow produced by the prototype unit.

ACKNOWLEDGEMENTS

This work was carried out under contract FIENI-DIMA 2014. The authors would like to thank Fieni S.r.l. for the possibility to work on this problem and would like to thank Alfredo and Alberto Melloni for the help in the workshop and the collaboration in this project.

REFERENCES

Chen, J. and Kevorkian, V., 1971, *Heat and Mass Transfer in Making Artificial Snow*, Ind. Eng. Chem. Process Des. Develop., Vol. 10, No. 1, 1971 75, DOI: 10.1021/i260037a014

Corsini, A., Rispoli, F., 2004, *Using sweep to extend stall-free operational range in axial fan rotors*, IMechE J. of Power and Energy, 218, 129-139, 2004.

Hanzer, F., Marke, T. and Strasser, U., 2014, *Distributed, explicit modeling of technical snow production for a ski area in the Schladming region (Austrian Alps)*, Cold Regions Science and Technology, Available online 21 August 2014, ISSN 0165-232X

Lagriffoul, A., Boudenne, J., Absi, R., Ballet, J., Berjeaud, J., Chevalier, S., Creppy, E. E., Gilli, E., Gadonna, J., Gadonna-Widehem, P., Morris, C. E. and Zini, S., 2010, *Bacterial-based additives for the production of artificial snow: What are the risks to human health*?, Science of The Total Environment, Volume 408, Issue 7, 1 March 2010, Pages 1659-1666, ISSN 0048-9697

Liao, J. C. and Ng, K.C., 1990, *Effect of ice nucleators on snow making and spray freezing*, Ind. Eng. Chem. Res., 1990, 29 (3), pp 361–366, DOI: 10.1021/ie00099a010

Lien, F.S. and Leschziner, M.A., 1994, Assessment of Turbulence-transport Models Including Non-linear RNG Eddy-viscosity Formulation and Second-moment Closure for Flow over a Backward-facing Step, Computers & Fluids, vol. 23, pp. 983-1004.

Sheard, A.G., Corsini. A., Minotti, S. & Sciulli, F., 2009, The Role of Computational Methods in the Development of an Aero-Acoustic Design Methodology: Application in a Family of Large Industrial Fans. Proceedings of the 14th International Conference on Modelling Fluid Flow Technologies. Budapest, Hungary, 9–12 September, pp 71–9.

Strub, M., Jabbour, O., Strub, F. and Bédécarrats, J. P., 2003, *Experimental study and modelling of the crystallization of a water droplet*, International Journal of Refrigeration, Volume 26, Issue 1, January 2003, Pages 59-68, ISSN 0140-7007.